

## Evidence against temperature chaos in mean-field and realistic spin glasses

This article has been downloaded from IOPscience. Please scroll down to see the full text article.

2000 J. Phys. A: Math. Gen. 33 L265

(<http://iopscience.iop.org/0305-4470/33/31/101>)

View [the table of contents for this issue](#), or go to the [journal homepage](#) for more

Download details:

IP Address: 171.66.16.123

The article was downloaded on 02/06/2010 at 08:29

Please note that [terms and conditions apply](#).

## LETTER TO THE EDITOR

**Evidence against temperature chaos in mean-field and realistic spin glasses**Alain Billoire<sup>†</sup> and Enzo Marinari<sup>‡</sup><sup>†</sup> CEA/Saclay, Service de Physique Théorique, 91191 Gif-sur-Yvette, France<sup>‡</sup> Dipartimento di Fisica and INFN, Università di Roma La Sapienza, P A Moro 2, 00185 Rome, Italy

Received 7 January 2000, in final form 2 May 2000

**Abstract.** We discuss temperature chaos in mean-field and realistic 3D spin glasses. Our numerical simulations show no trace of a temperature chaotic behaviour for the system sizes considered. We discuss the experimental and theoretical implications of these findings.

(Some figures in this article are in colour only in the electronic version; see [www.iop.org](http://www.iop.org))

The problem of chaos in spin glasses has been under investigations for many years [1–9]. Even in the Sherrington–Kirkpatrick (SK) model, which is well understood with the Parisi solution of the mean-field theory [10], the possible presence or absence of temperature chaos is still an open problem. In contrast, for example, chaos induced by a magnetic field  $h$  was discussed by Parisi [1] 15 years ago, and it is a clear feature of the replica symmetry breaking (RSB) scenario. We will give here numerical evidence of the fact that, for all lattice sizes we are able to investigate by using a state of the art optimized Monte Carlo method (see e.g. [11]), there is no trace of temperature chaos in mean-field (infinite-range) and realistic spin glasses, in contradiction with previous claims [2,5–9]. The question of temperature chaos can be phrased by considering a typical equilibrium configuration at temperature  $T$ , and one (under the same realization of the quenched disorder) at  $T' = T + dT$ , where  $dT$  is small: how similar are two such configurations? In a chaos scenario for any non-zero  $dT$  the typical overlap would be exponentially small in the RSB approach and decreasing as a power in the droplet approach as a function of the system size. We study both SK and diluted mean-field (DMF) [12] models. We consider the DMF model in its version with constant connectivity  $c = 6$ . Each lattice site is connected to  $c$  other sites chosen at random. It is interesting to check whether this model has the same features as the SK model. We also study the 3D Edwards–Anderson (EA) realistic spin glass. In all models spin variables are Ising like ( $\sigma = \pm 1$ ), and the couplings  $J$  can take the two values  $\pm 1$  with probability  $\frac{1}{2}$ . Our Monte Carlo dynamics is based on parallel tempering (PT) [11]: we run in parallel two sets of copies of the system, and always take the overlap of configurations from two different Markov chains. We use all standard precautions for checking the thermalization of our data [11]. The indicator of a potential chaotic behaviour will be the two-temperature overlap  $q_{T',T}^{(2),(N)} \equiv \langle (\frac{1}{N} \sum_{i=1}^N \sigma_i^{(T)} \tau_i^{(T')})^2 \rangle$ . The usual square overlap  $q_{T,T}^{(2),(N)}$  is a special case of  $q_{T',T}^{(2),(N)}$ .

Let us start from the analysis of our data for the SK model. In figure 1 we plot the square overlap for the two temperature values  $(0.4, T)$  (i.e. the overlap of a copy of the system at

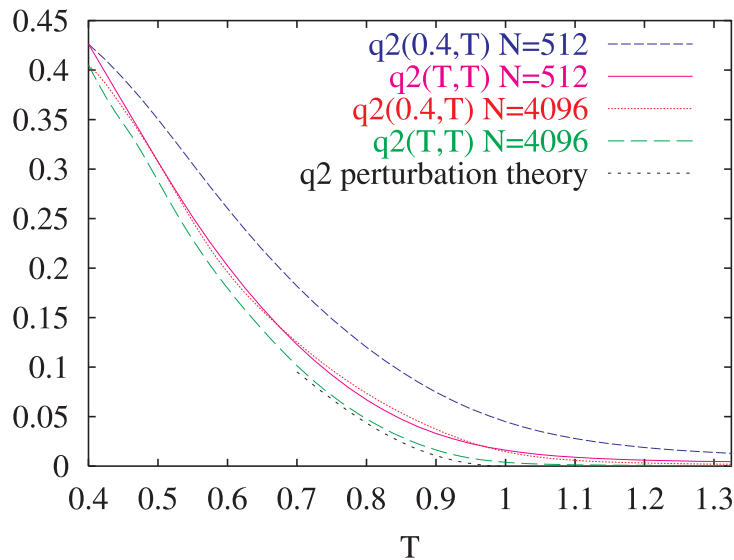


**Figure 1.**  $q^{(2)}$  at equal and different  $T$  values for the SK model, with  $N = 512$  and  $4096$  sites. The lower curve is the perturbative result for equal  $T$   $q^{(2)}$ . See the text for details.

temperature  $T' = 0.4$  with a copy of the system at  $T \in (0.4, 1.35)$ ), and the one at equal temperature  $(T, T)$ . The two upper (on the left side of the plot) dashed curves (merging at  $T = 0.4$  at a value close to 0.42) are for  $N = 512$  spins (a small lattice size), the upper one being the  $(0.4, T)$  curve and the lower one the  $(T, T)$  one. The two lower curves (merging at  $T = 0.4$  at a value close to 0.40) are for  $N = 4096$  (our largest lattice for the SK model): of these two lower curves, the solid upper curve is for  $(0.4, T)$ , while the dashed lower one is the  $(T, T)$   $q^{(2)}$ . The fifth curve from the top, that stops at  $T = 0.7$ , is the perturbative result for  $q_{T,T}^{(2),(\infty)}$  [13] (useful for checking our numerics and the quality of the approach to the asymptotic large-volume limit). Here we only plot data from two lattice sizes, and do not show the statistical errors, that are small enough not to affect any of the issues discussed here, but would make the picture less readable. We show data for the lowest temperature we have been able to thermalize,  $T' = 0.4$ . The same qualitative picture holds for larger  $T'$  values ( $T' < T_c$ ).

One notices at first glance from figure 1 that for both  $N$  values (and, as we will see, for all  $N$  values and different systems we have analysed)  $q_{0.4,T}^{(2),(N)} \gtrsim q_{T,T}^{(2),(N)}$  ( $T \geq 0.4$ ). This is what happens in non-chaotic systems (for example ferromagnets, where  $q_{T',T}^{(2),(N)} = M(T)^2 M(T')^2$ , where  $M(T)$  is the magnetization at temperature  $T$ ), and is very different from what would happen in a system with  $T$ -chaotic states. The second crucial observation is that the distance between  $q_{0.4,T}^{(2),(N)}$  and  $q_{T,T}^{(2),(N)}$ , at fixed  $T > 0.4$ , decreases with  $N$ : the two curves even seem to collapse at large  $N$ . This kind of behaviour shows the absence of temperature chaos in the SK system and, as we will discuss in the following, in the DMF and 3D EA spin glasses. This evidence, together with an understanding of the physical mechanism that is at the origin of this behaviour (thanks to the analysis of  $P(q)$ ), is the main point of this letter.

More quantitative evidence comes from figure 2, where we plot  $q_{0.4,T}^{(2),(N)} - q_{T,T}^{(2),(N)}$  as a function of  $T$  for the SK model with  $N = 256, 512, 1024, 2048$  and  $4096$ . Here the errors are computed by an analysis of sample-to-sample fluctuations (it is important not to forget that the points for different temperatures are strongly correlated, since they involve the same  $T = 0.4$

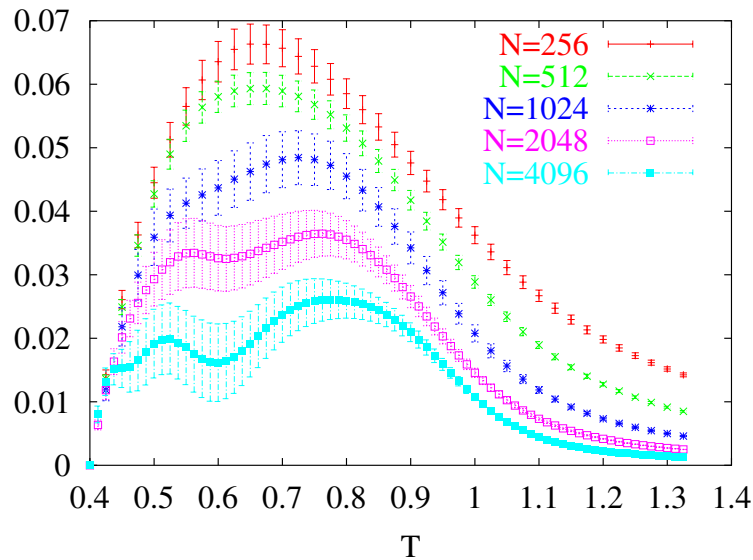


**Figure 2.**  $q_{0.4,T}^{(2),(N)} - q_{T,T}^{(2),(N)}$  as a function of  $T$  for the SK model with different  $N$  values.

data, or data from different temperatures but nevertheless from the same PT simulation). In the large-volume limit both contributions to the difference are zero for  $T > T_c = 1$ , so the non-zero value of the curves in this regime gives us a measure of finite-size effects. Large lattices have larger fluctuations. This is connected to the non-self-averagedness of  $P_J(q)$ : the peaks of  $P_J(q)$  become narrower for large lattices (eventually approaching  $\delta$ -functions in the large-volume limit), and averaging them to compute expectation values of the overlap gives a wiggling behaviour, that becomes smooth only for a very large number of disorder samples. We are not able to keep under control a precise fit of the data of figure 2 for  $N \rightarrow \infty$ , but the strong decrease of the difference of the data at large  $N$  is clear, and the possibility that the limit is zero everywhere looks very plausible (it would be very interesting to understand this behaviour theoretically).

We use figure 3 to try to understand better the mechanism governing how stable states of the system vary as a function of  $T$ . We plot the probability distribution  $P_J(q)$  for a given disorder realization of the SK model with  $N = 4096$ . We show, from top to bottom, the results at  $T = 0.50, 0.45$  and  $0.40$ . The function  $P_J(q)$  should be symmetric around  $q = 0$ , since we are at zero magnetic field. The level of symmetry reached by our finite-statistics sample is a measure of the quality of our thermalization: from figure 3 it looks very good. Note that there is no peak close to, or at, the origin: this disorder realization carries little weight in the  $q \simeq 0$  region. At the lowest  $T$  value there are five peaks for positive  $q$ , three of which are very well separated. It is interesting to follow the evolution of  $P_J(q)$  from  $T = 0.50$  down to  $0.40$ . At  $T = 0.50$  there are basically two very broad peaks, that become resolved at  $T = 0.45$ : one broad peak is divided into two clear peaks (that become very clear at  $T = 0.4$ ), while the other forms a three-peak structure, that have different weights at  $T = 0.4$ . What one sees in figure 3 is interesting since it constitutes a typical pattern: when lowering  $T$ , states start to contribute to the  $P_J(q)$  by bifurcations (new peaks emerge) and by smooth rearrangements of the weights. One never sees dramatic changes involving strong redistributions of weight among far-away peaks, that would be typical of a chaotic situation: the phase space is obviously very complex,

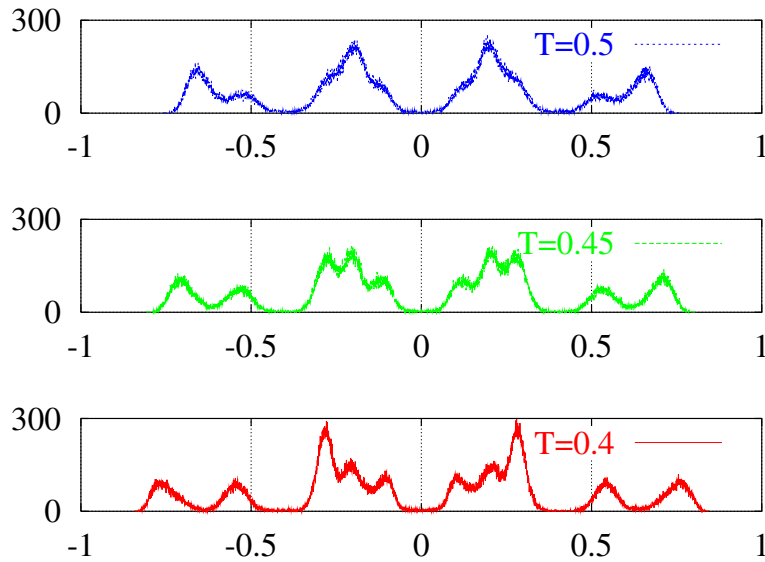


**Figure 3.**  $P_J(q)$  for the same selected disorder realization at three different temperatures of the SK model with  $N = 4096$  sites.

as it has to be in a situation characterized by RSB [10], but the  $T$  dependence of the phase space is smooth and non-chaotic.

The situation in the DMF model (where  $T_c \simeq 2.07$ ) is very similar to the one in the SK model. In figure 4 we show the analogue of figure 2, for  $N = 64, 512$  and  $4096$  spins. The two figures are very similar, and even the size of the difference we are plotting is very similar in the two models, when comparing the same values of  $N$ . The situation in the DMF model looks exactly the same as that in the SK model: there is no temperature chaos.

The situation in the 3D EA model is different only in that finite-size effects are very large (this is well known from numerical simulations [14]). In figure 5 we show  $q^{(2)}$  at equal and different  $T$  values for  $L = 4, 8$  and  $16$ . It is clear that  $q^{(2),(N)}$  decreases noticeably with  $N = L^3$  for all values of  $T$ . It is also remarkable that even at very large  $T$  values (with  $T$  far larger than the estimated value of  $T_c \simeq 1.16$  [15, 16])  $q^{(2),(N)}$  is different from zero even at  $N = 4096 = 16^3$ . Apart from that figure 5 shows a situation very similar to that of figure 1. We are definitely not in a situation where  $q_{0.4,T}^{(2),(N)}$  goes to zero exponentially or as a power and  $q_{T,T}^{(2),(N)}$  goes to a non-zero limit (even if the distance between the two curves for  $L = 16$  has become very small, and even negative in a certain temperature region). In figure 6 we show the 3D analogue of figures 2 and 4. Again, even for  $T > T_c$ , on the smaller lattices one has non-zero differences: finite-size effects are large, but apart from that the emerging picture is analogous to the one we have found in the mean field (diluted and not). We want to stress that in the 3D case one has to be even more careful since the lower critical dimension is very close, and transient effects could be very misleading.

Now, before discussing the data, we give a few details about our runs. For the SK model we use  $T_{\min} = 0.4 = 0.4T_c$ . We simulate  $N = 256, 512, 1024, 2048$  and  $4096$ : for the different- $N$  cases we have from 26 to 142 samples, a set of from 38 to 75 temperature values with a  $dT$  from 0.025 to 0.0125. We run 200 000 sweeps except for the  $N = 4096$  and  $2048$  lattices, where we run 400 000 sweeps (we always use for measurement only the second part of the run). For the DMF model we have  $T_{\min} = 0.8 \simeq 0.4T_c$ . We use from 640 to 1024

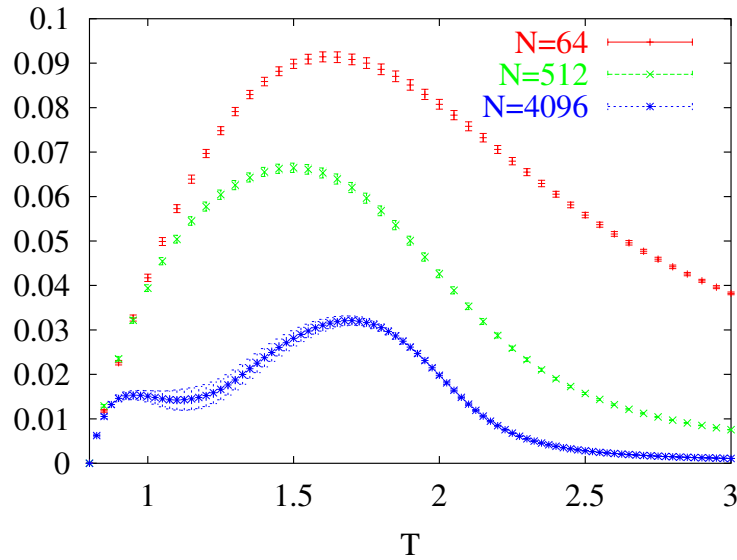


Figure 4. As in figure 2, but for the DMF model,  $N = 64, 512$  and  $4096$ .

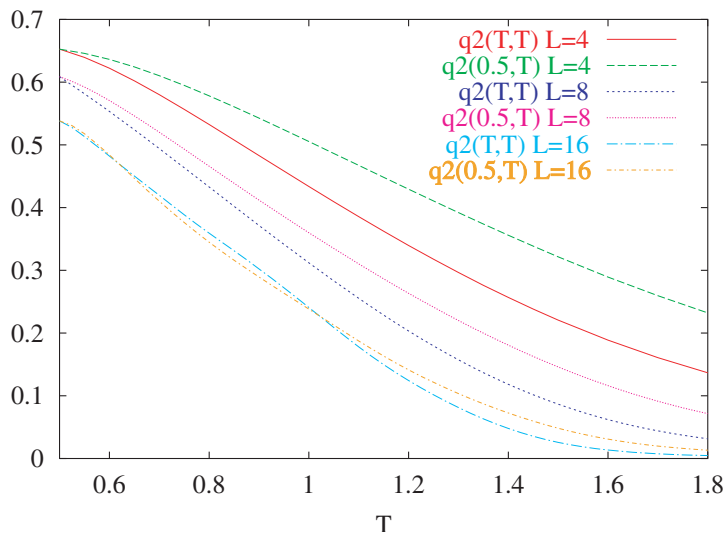
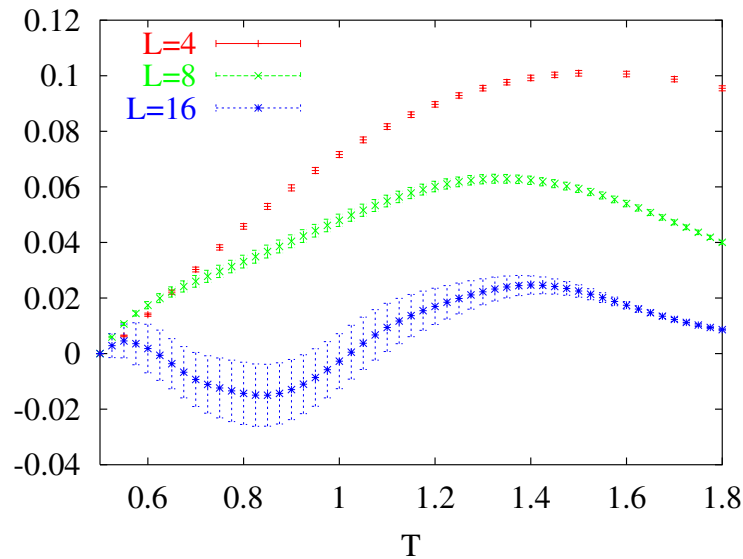


Figure 5.  $q^{(2)}$  at equal and different  $T$  values for the 3D EA model.

samples for  $N = 64, 512$  and  $4096$ . Here  $T_{\max}$  is 3, the number of temperatures from 45 to 89 and the number of iterations from 100 000 to 200 000. In the 3D EA model we use  $T_{\min} = 0.4$ ,  $T_{\max} = 2.075$  (here  $T_c \simeq 1.16$ ) and a  $dT$  from 0.050 to 0.025. We have 1344 samples for  $L = 4$  (200 000 sweeps) and 8 (300 000 sweeps), and 64 samples for  $16^3$  (where  $T_{\min} = 0.5$ , with 3450 000 sweeps; this is very many sweeps of many tempering copies). Our SK program was multi-spin coded on different sites of the same system (we store 64 spins of the system in the same word), while the DMF and 3D codes are multi-spin coded on different copies of



**Figure 6.**  $q_{0.5,T}^{(2),(N)} - q_{T,T}^{(2),(N)}$  as a function of  $T$  for the 3D EA model with different  $L$  values.

the system [17]†. We want to note that, as compared with previous numerical simulations, we have been able (thanks to a large computational effort and to the use of PT) to thermalize the systems at very low  $T$  values. It is also interesting to notice that in the  $N = 4096$  case the 3D EA model requires many more sweeps than the DMF and the SK model.

In all our simulations we do not observe any temperature chaos effect. This is true for the SK model, the DMF and the 3D EA model: the three models behave very similarly. The differences we have plotted, that would decrease exponentially in a RSB chaotic scenario, do not decrease faster than logarithmically. Obviously from our numerical findings we cannot be sure that things will not change for very large system sizes, but, again, we can claim that the absence of any temperature chaotic behaviour is crystal clear on our lattice size. Two final comments are in order. First, as we have already said, we cannot be sure about the behaviour in the very-large-system limit: the difference between  $q_{T',T}^{(2)}$  and  $q_{T,T}^{(2)}$  (for  $T' \simeq 0.4T_c$  and  $T > T'$ ) decreases with the system volume, and is close to zero on the larger lattice sizes we can simulate. This difference could eventually become negative, and the correlation at  $T \neq T'$  could eventually drop faster on very large lattices: we can only say we do not see any trace of that. The second comment is that, in any case, our results have an experimental relevance: the number of spins that are equilibrated during a real experiment is of an order of magnitude only slightly larger than the order of magnitude of the one we can thermalize in our numerical simulations [18], so our results strongly suggest the absence of temperature chaos in real experiments.

The previous work of other authors on chaos was pointing toward the presence of temperature chaos. On one hand in this context the analytic computations have by no means an unambiguous meaning, since they are based on strong assumptions or on a perturbative and/or approximate treatment. On the other hand numerical computations of older generations were much limited in scope as compared with what we can do now. For example, Ritort numerical computation [7], that correctly, in the limit of the gathered data, found chaos, used a  $T$  starting

† Our code is based on the unpublished work of F Zuliani (1998).

value of 0.4, and a  $dT$  of 0.5 (as compared with the value of 0.0125 we have been able to use here), i.e. was comparing  $T = 0.4$  with 0.9 (where  $T_c = 1$ ) on a reasonably small lattice. In this case the decrease of the overlap is clear, but turns out to be due to the finite-size effect (since even the equal  $T$  overlap has to go to zero at  $T_c$ ).

One further word of caution (together with the caveat we have already issued) is appropriate: it is clear that in order to obtain reliable evidence about the presence or the absence of chaos we need to be able to measure in an appropriate window of temperature jumps. Too large a jump would surely make the measurement biased from the presence of  $T_c$ , while too small a jump would not allow the overlap length to be small enough to be measured. These conflicting criteria can represent a potential problem with the interpretation of the data.

A last comment (following, for example, [19]) concerns the relevance of the absence of chaos for the description of realistic, finite-dimensional spin glasses. In short the absence of a temperature chaotic behaviour makes a modified droplet-like description of realistic spin glasses impossible (the original droplet model cannot work, for example, because of the observed dynamical scaling of the energy barriers).

Following [19] one notices that the very weak dependence of spin glass physical properties on the cooling rate is not plausible in a scenario of activated domain growth. Only arguing that there is temperature chaos can one reconcile the negligible effect of the cooling rate with a droplet picture. The absence of temperature chaos makes this reconciliation impossible.

We are aware that G Parisi and T Rizzo in a perturbative computation close to  $T_c$  find absence of temperature chaos (at the order they compute, but not necessarily at all orders in perturbation theory), both in the SK and DMF models. S Franz and I Kondor have connected evidence that excludes temperature chaos at lowest orders close to  $T_c$ . We deeply thank all of the above, together with J-P Bouchaud and F Ritort, for interesting conversations. The numerical simulations have used, together with a number of workstations, computer time from the Grenoble T3E Cray and the Cagliari Linux cluster Kalix2 (funded by the Italian MURST under a COFIN grant).

## References

- [1] Parisi G 1984 *Physica A* **124** 523
- [2] Bray A J and Moore M A 1987 *Phys. Rev. Lett.* **58** 57
- [3] Binder K and Young A P 1986 *Rev. Mod. Phys.* **58** 801
- [4] Kondor I 1989 *J. Phys. A: Math. Gen.* **22** L163
- [5] Ney-Nifle M and Hilhorst H J 1993 *Physica A* **193** 48
- [6] Kondor I and Végö A 1993 *J. Phys. A: Math. Gen.* **26** L641
- [7] Ritort F 1994 *Phys. Rev. B* **50** 6844
- [8] Franz S and Ney-Nifle M 1995 *J. Phys. A: Math. Gen.* **28** 2499
- [9] Ney-Nifle M 1998 *Phys. Rev. B* **57** 492  
(Ney-Nifle M 1997 *Preprint cond-mat/9707172*)
- [10] Mézard M, Parisi G and Virasoro M A 1987 *Spin Glass Theory and Beyond* (Singapore: World Scientific)
- [11] Marinari E 1998 *Advances in Computer Simulation* ed J Kerstéz and I Kondor (Berlin: Springer) p 50  
(Marinari E 1996 *Preprint cond-mat/9612010*)
- [12] Banavar J R, Sherrington D and Surlas N 1987 *J. Phys. A: Math. Gen.* **20** L1  
Mézar M and Parisi G 1987 *Europhys. Lett.* **3** 1067
- [13] Sommers H J 1985 *J. Physique* **46** L779
- [14] Marinari E, Parisi G and Ruiz-Lorenzo J 1998 *Spin Glasses and Random Fields* ed P Young (Singapore: World Scientific) p 59  
(Marinari E, Parisi G and Ruiz-Lorenzo J 1997 *Preprint cond-mat/9701016*)
- [15] Kawashima N and Young A P 1996 *Phys. Rev. B* **53** R484  
(Kawashima N and Young A P 1995 *Preprint cond-mat/9510009*)



- [16] Palassini M and Caracciolo S 1999 *Phys. Rev. Lett.* **82** 5128  
(Palassini M and Caracciolo S 1999 *Preprint* cond-mat/9904246)
- [17] Rieger H 1993 *J. Stat. Phys.* **70** 1063  
(Rieger H 1992 *Preprint* hep-lat/9208019)
- [18] Joh Y G *et al* 1999 *Phys. Rev. Lett.* **82** 438  
(Joh Y G *et al* 1998 *Preprint* cond-mat/9809246)
- [19] Bouchaud J-P, Cugliandolo L F, Kurchan J and Mézard M 1998 *Spin Glasses and Random Fields* ed P Young  
(Singapore: World Scientific) p 161